

University of Nebraska - Lincoln

DigitalCommons@University of Nebraska - Lincoln

Anthony F. Starace Publications

Research Papers in Physics and Astronomy

10-2011

Attosecond Streaking in the Low-Energy Region as a Probe of Rescattering

Ming-Hui Xu
Peking University

Liang-You Peng
Department of Physics and State Key Laboratory for Mesoscopic Physics, Peking University, Beijing,
liangyou.peng@pku.edu.cn

Zheng Zhang
Peking University

Qihuang Gong
Department of Physics and State Key Laboratory for Mesoscopic Physics, Peking University, Beijing,
qhong@pku.edu.cn

Xiao-Min Tong
University of Tsukuba, Japan, tong@ims.tsukuba.ac.jp

See next page for additional authors

Follow this and additional works at: <https://digitalcommons.unl.edu/physicsstarace>

 Part of the [Physics Commons](#)

Xu, Ming-Hui; Peng, Liang-You; Zhang, Zheng; Gong, Qihuang; Tong, Xiao-Min; Pronin, Evgeny A.; and Starace, Anthony F., "Attosecond Streaking in the Low-Energy Region as a Probe of Rescattering" (2011). *Anthony F. Starace Publications*. 187.
<https://digitalcommons.unl.edu/physicsstarace/187>

This Article is brought to you for free and open access by the Research Papers in Physics and Astronomy at DigitalCommons@University of Nebraska - Lincoln. It has been accepted for inclusion in Anthony F. Starace Publications by an authorized administrator of DigitalCommons@University of Nebraska - Lincoln.

Authors

Ming-Hui Xu, Liang-You Peng, Zheng Zhang, Qihuang Gong, Xiao-Min Tong, Evgeny A. Pronin, and Anthony F. Starace

Attosecond Streaking in the Low-Energy Region as a Probe of Rescattering

Ming-Hui Xu,¹ Liang-You Peng,^{1,*} Zheng Zhang,¹ Qihuang Gong,^{1,†} Xiao-Min Tong,^{2,‡}
Evgeny A. Pronin,³ and Anthony F. Starace^{3,§}

¹State Key Laboratory for Mesoscopic Physics and Department of Physics, Peking University, Beijing 100871, China

²Institute of Materials Science, University of Tsukuba, Ibaraki 305-8573, Japan

³Department of Physics and Astronomy, The University of Nebraska, Lincoln, Nebraska 68588-0299, USA

(Received 22 February 2011; revised manuscript received 31 August 2011; published 26 October 2011)

The dynamics of low-energy photoelectrons (PEs) ionized by a single attosecond pulse in the presence of an intense infrared (IR) laser field is investigated. Whereas attosecond streaking usually involves momentum shifts of high-energy PEs, when PEs have low initial kinetic energies, the IR field can control the continuum-electron dynamics by inducing PE scattering from the residual ion. A semiclassical model is used to show that particular PE trajectories in the continuum involving electron-ion scattering explain the interference patterns exhibited in the low-energy PE spectrum. We confirm the effects of the trajectories by means of a full quantum simulation.

DOI: 10.1103/PhysRevLett.107.183001

PACS numbers: 33.20.Xx, 03.65.Sq, 34.50.Rk, 42.25.Hz

The rescattering process [1,2] in strong field physics leads to many phenomena from which structural and dynamical information on the target system can be extracted. Recently, photoelectrons (PEs) undergoing laser-driven recollision were utilized to retrieve such information for both atoms [3] and molecules [4]. Very recently, an analysis of high-order harmonic generation (HHG) (from the photorecombination of returning electrons ionized from aligned N₂ molecules) was shown to provide experimental images of the attosecond (as) wave packet created in the initial ionization process [5]. An underlying premise of such imaging is knowledge or control of the continuum electron's trajectories in the strong infrared (IR) laser field. Thus, in Ref. [3], only the most energetic PEs were used in the analysis owing to the simplicity of their trajectories. Also, in Ref. [5], only short electron trajectories were selected for the tomographic reconstruction of the molecular orbital. In general, however, the dynamics of a continuum electron in the combined fields of both a strong IR laser field and an atomic or molecular potential is quite complicated. In particular, higher-order return trajectories have been shown to play an important role in above threshold ionization [6] and in HHG [7]. Control of the continuum-electron dynamics, moreover, is difficult when both the initial ionization of the active electron and its further acceleration in the continuum are governed by the same strong IR laser field.

The use of an IR field to assist ionization of atoms by an extreme ultraviolet (XUV) attosecond pulse train (APT) has been actively investigated (see, e.g., Refs. [8–12]). By fixing the phase of the IR field relative to the XUV APT, ionization of electrons can be controlled and information on transiently bound states can be obtained. Owing to the use of APTs, the bandwidth of the XUV-produced electron spectrum is quite narrow (typically $\ll 1$ eV [12]). Interpretation of the results is complicated owing to the

many electron wave packets produced by the APT. A similar investigation of picosecond IR laser ionization of the Li atom in the presence of a microwave field has recently been carried out [13]. Note that control of ionization is not limited to the use of an APT. Very recently, a study of multiphoton ionization of He by long two-color XUV pulses in the presence of an IR field showed how ionization amplitudes can be controlled to produce electromagnetically induced transparency in the XUV regime [14].

The production of single attosecond pulses (SAPs) [15–17] in the XUV regime enables a new class of experiments, in which a *broadband* electron wave packet is created in the continuum by a SAP and then steered by a synchronized IR field with stabilized carrier-envelope phase [18]. This decoupling of the creation and acceleration of continuum electrons provides a remarkable degree of control over electron motion. For PEs with high initial momenta, interaction with the parent ion can be ignored; the IR field thus simply shifts PE momenta by $\mathbf{A}_L(t_i)$, the IR field's vector potential at the time of ionization t_i [19]. Attosecond streaking, which is based on this principle, has enabled measurements of electron dynamics with a time resolution approaching the atomic unit of time [20].

In this Letter, we investigate the rescattering of low-energy PEs resulting from ionization by a few-cycle (and hence broadband) SAP in the presence of an IR laser field that is intense enough to deflect some of the PEs so that they revisit the parent ion one or more times. By analyzing the resulting interference patterns in the PE spectrum along the direction of laser polarization, we are able to identify the most important continuum-electron trajectories, thus elucidating the rescattering process. For a short IR laser pulse, we find that interference can occur between direct outgoing electrons and backscattered ones; also a hump structure may occur due to low-energy forward scattering. For a longer IR pulse, higher-order returns

manifest themselves by spectra having more complex interference patterns, e.g., with substructures. Low-energy attosecond streaking is thus shown to provide an ideal means to study and control rescattering electron dynamics in the field of an ion. These results indicate the potential of such broadband XUV + IR field investigations of rescattering phenomena for holographic imaging of atoms and molecules, in which the target is “scanned” by the rescattered electrons and the directly ionized electrons serve as a “reference” beam.

We solve the time-dependent Schrödinger equation (TDSE) numerically for a He atom interacting with a SAP and an IR laser pulse, with both assumed to be linearly polarized and to overlap temporally. Within the single-active electron approximation, the TDSE (in atomic units, a.u.) is

$$i \frac{\partial}{\partial t} \psi(\mathbf{r}, t) = \left[-\frac{1}{2} \nabla^2 + V(r) + H_I(t) \right] \psi(\mathbf{r}, t), \quad (1)$$

where $V(r)$ is a model potential [21] that reproduces the He ionization potential to an accuracy of 10^{-3} . We solve Eq. (1) in both length gauge and velocity gauge (to check consistency), with $H_I(t) = \mathbf{r} \cdot \mathbf{E}(t)$ or $\mathbf{p} \cdot \mathbf{A}(t)$ respectively, where $\mathbf{E}(t)$ is the sum of the electric fields of the SAP and IR pulse and $\mathbf{A}(t)$ is the corresponding vector potential. Since we focus on low-energy PEs, we employ a SAP similar to that produced in Ref. [15], i.e., 126 as (full width at half maximum) with a central frequency of 36 eV, but having a slightly higher peak intensity of 10^{12} W/cm². For our low-energy attosecond streaking investigation, the SAP is placed at a zero of the IR laser electric field, which results in the maximum momentum shift of the electron that is promoted to the continuum by the SAP from the initial state. The IR laser intensity is chosen to be too weak to affect the bound electron, but strong enough to steer continuum electrons. The spatial discretization and the time evolution of the TDSE follow the recommendations of Ref. [22]: The grid spacing is 0.05 a.u. and the time step is 0.02 a.u. The PE spectra are obtained by projecting the final wave function onto energy eigenstates of the field-free Hamiltonian that satisfy the incoming wave boundary condition [23]. Note that unlike investigations of low-energy electrons produced by an APT in the presence of an IR field, our use of a SAP results in a *broadband* initial ionized electron momentum distribution, providing greater opportunity for different IR field-induced interference phenomena. Since the central frequency of our SAP is rather far above the ionization threshold, the probability for excitation of Rydberg states is found to be <15% of the ionization probability; i.e., they do not play a large role in the phenomena described below.

Consider first a 2-cycle IR laser pulse (with $\lambda = 750$ nm and $I_0 = 2 \times 10^{13}$ W/cm²) having a trapezoidal envelope comprised of a one-cycle flat top and a half-cycle turn on and turn off, as shown in Fig. 1(a). [Note that use of a

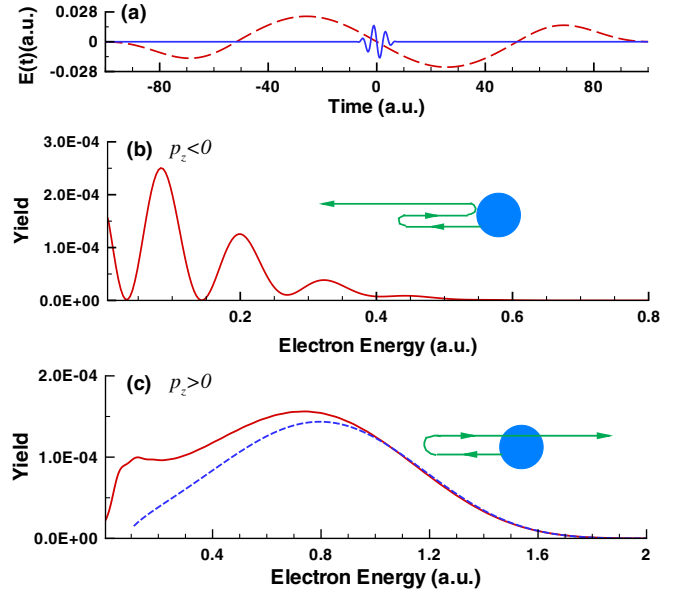


FIG. 1 (color online). (a) Electric fields of the SAP [solid (blue) line, multiplied by a factor of 3] and the 2-cycle IR pulse [dashed (red) line]. Energy spectra of PEs ionized from He along the laser field polarization axis: (b) $p_z < 0$ and (c) $p_z > 0$. Insets in (b) and (c) illustrate schematically PE trajectories that are initially ejected by the SAP with $p_z(0) < 0$, but are decelerated and at a later time experience, respectively, backward or forward rescattering. The dashed (blue) line in (c) is the PE spectrum produced by the SAP pulse in which the PE momenta are simply shifted by the IR vector potential; see text for details.

Gaussian pulse shape gives qualitatively similar numerical results, but the results are easier to analyze for a trapezoidal pulse shape.] For the SAP and IR pulse intensities chosen, ionization is almost entirely due to the SAP, while the IR field only affects the motion of PEs ionized by the SAP. The photoelectron energy spectra resulting from ionization of He by the SAP in the presence of the IR pulse for photoelectrons having negative ($p_z < 0$) and positive ($p_z > 0$) momenta along the laser polarization axis are shown, respectively, by the solid (red) lines in Figs. 1(b) and 1(c). One observes two distinctive features of the PE spectrum: (1) An oscillatory pattern for $p_z < 0$ [Fig. 1(b)]; (2) A hump structure at low energies for $p_z > 0$ [Fig. 1(c)]. We show below that reencounters of some PEs with the He⁺ ion are responsible for these two features.

To explain the oscillation patterns, we employ a simple semiclassical model in terms of trajectories [24]. First, consider the classical trajectories of PEs that are initially ejected by the SAP with momenta $p_z(0) < 0$ along the laser polarization axis. After ionization, they are decelerated by the IR field. So whereas the low kinetic energy part of these PEs will reverse direction and revisit the helium ion at a later time [25], the high-energy (direct) part simply quivers away with reduced negative momentum. If backscattering occurs [Fig. 1(b), inset], the final energies of the backscattered electrons and those direct electrons having

the same negative momentum will overlap; i.e., interference occurs between these two pathways (direct and backscattered). Second, the oscillations due to interference are controlled by the time evolution phase. The quantum phase acquired by a free electron in an electromagnetic field is given by the Volkov phase, $e^{-iS_p(t)}$, where $S_p(t)$ denotes the semiclassical action of the trajectory,

$$S_p(t) = \frac{1}{2} \int_0^t d\tau [\mathbf{p} + \mathbf{A}_L(\tau)]^2, \quad (2)$$

with $\mathbf{p} + \mathbf{A}_L$ being the classical momentum of the PE. The reflected electrons are found (see below) to obtain an additional phase of π upon reflection (analogous to the $\lambda/2$ phase change upon reflection in optics). We assume that the reflection probability equals unity. Despite the simplicity of this semiclassical model of two interfering pathways for photoelectrons having $p_z < 0$, this model reproduces the frequency of the oscillations (i.e., the spacing between adjacent peaks) very well over a wide range of energies [cf. Fig. 2(a)]. (Qualitatively, one expects the agreement to improve for longer wavelengths owing to the greater quiver amplitude.) The exact *positions* and *amplitudes* of the interference fringes, of course, require knowledge of the quantum reflection probability. Our simple model's success indicates that the interference *spacings*

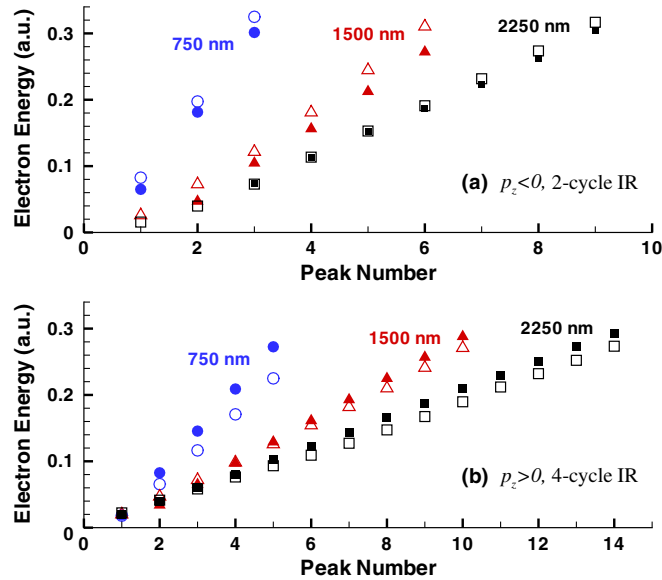


FIG. 2 (color online). Comparisons of peak positions (plotted vs peak number above threshold) of the interference pattern in the PE spectrum for: (a) $p_z < 0$ and 2-cycle IR pulse case [cf. Fig. 1(b)]; (b) $p_z > 0$ and 4-cycle IR pulse case [cf. Fig. 3(b)]. In each frame, TDSE results (open symbols) are compared with predictions of the semiclassical model (filled symbols). The wavelengths and intensities of the IR laser are: $\lambda = 750$ nm and $I_0 = 2 \times 10^{13}$ W/cm² (circles); 1500 nm and $I_0/4$ (triangles); 2250 nm and $I_0/9$ (squares). Thus the peak vector potentials of the IR pulses remain the same in each case. Finally, the SAPs are the same in all cases.

depend largely on the IR laser pulse. Note also that the interference between the direct PEs and the backscattered ones is similar to that in optical holography. The reflected PEs carry information about the parent ion in the scattering process. And the direct PEs serve as the reference wave. Therefore, the interference pattern can be viewed as an electron hologram, within which information on the parent ion is encoded.

Consider now the PE spectrum in Fig. 1(c). Upon ionization by the SAP, a PE having an initial momentum $p_z(0) > 0$ along the laser polarization axis will then be accelerated by the first half-cycle of the remaining single cycle of the IR field and will not revisit the helium ion. If we ignore the effect of the He ion potential on the PE, the final momentum of the PE will be shifted to a larger positive momentum, with the shift given by the vector potential of the IR laser pulse at the time of ionization (cf. the analysis in Ref. [19]). We illustrate the prediction of such a model for the PE spectrum by the dashed (blue) line in Fig. 1(c), which is the result of shifting the momentum spectrum of PEs ionized from the He atom by the SAP pulse alone, with the shift equal to the peak vector potential of the IR laser pulse [26]. Not surprisingly, the agreement between the TDSE result and the momentum-shift prediction is remarkable for PEs with energies higher than 1 a.u. However, for lower energy PEs, the agreement is poor, because the ionic potential plays an important role that cannot be ignored. Interestingly, a hump structure below 0.3 a.u. appears in the spectrum. As discussed above, in the PE spectrum for $p_z < 0$, backscattering of PEs leads to the interference structures shown in Fig. 1(b). However, some of the PEs with initial momenta $p_z(0) < 0$ can undergo forward scattering [cf. the inset in Fig. 1(c)]. Such low-energy forward scattering contributes to the hump structure of the PE spectrum for $p_z > 0$. Our TDSE calculations further indicate that the significance of the hump structure increases as the IR laser wavelength and intensity increase. Thus, this hump structure is reminiscent of the unexpected low-energy structure found in the PE spectrum produced by an intense mid-IR laser [27,28].

To explore attosecond streaking at low energies further, we increase the duration of the IR laser pulse to 4 cycles [see Fig. 3(a)], with a pulse envelope comprised of a 3-cycle flattop and a half-cycle turn on and turn off; all other laser parameters are the same as for those in Fig. 1. Comparisons of the PE spectra for the 4-cycle IR laser [solid (red) lines] with those for the 2-cycle IR laser [dashed (blue) lines] are given in Figs. 3(b) and 3(c). For the $p_z > 0$ spectrum in Fig. 3(c), oscillations with a spacing of one IR photon energy appear in the low-energy region. In applying our semiclassical model to analyze this spectrum, one expects that classical trajectories for low-energy PEs are more complicated for longer IR pulses [29]. Thus, e.g., some PEs experiencing forward scattering [Fig. 1(c) inset] may revisit the ion a second time under the

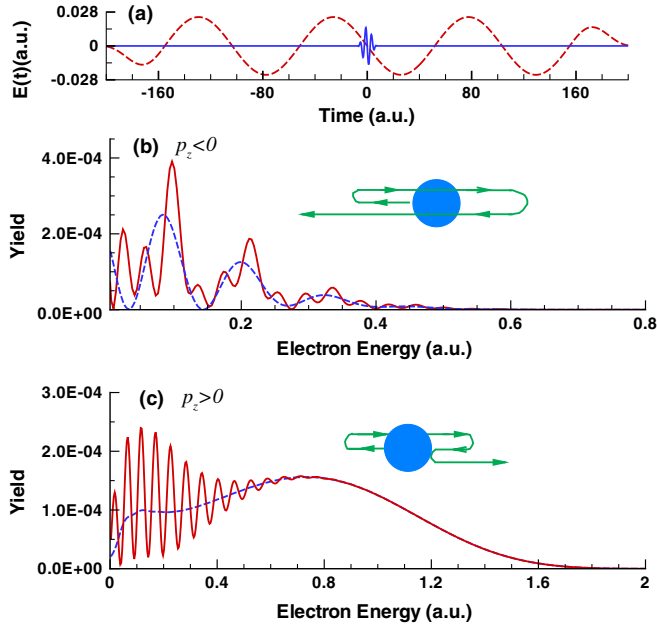


FIG. 3 (color online). Same as Fig. 1, but with a 4-cycle IR laser. The dashed (blue) lines in (b) and (c) are the PE spectra for the 2-cycle IR case, as shown in Figs. 1(b) and 1(c) respectively. Insets in (b) and (c) illustrate schematically PE trajectories involving two rescatterings.

influence of a 4-cycle IR pulse. If backscattering occurs at the second encounter, these (forward and then backscattered) PEs [Fig. 3(c) inset] can interfere with both the forward-scattering-only PEs [Fig. 1(c) inset] and the PEs initially emitted with $p_z(0) > 0$. As shown in Fig. 2(b), the energy separations of the interference structures in the PE spectrum in Fig. 3(c) can be reproduced quite accurately by the semiclassical model, thus explaining their origin as due to interference between three different continuum PE quantum trajectories.

The influence of higher-order electron trajectories on the PE spectrum for $p_z < 0$ is also evident. As shown in Fig. 3(b), for the 4-cycle IR laser pulse case substructures appear on the interference peaks observed in the 2-cycle IR laser case. This indicates that additional PE trajectories with lower amplitudes contribute to the interference between the directly ionized and the backscattered PEs. In the inset of Fig. 3(b), we show one such possible higher-order trajectory in which PEs experience forward scattering from the He^+ ion twice.

To confirm the above semiclassical trajectory interference explanation, we have performed another TDSE calculation in which we solve the time-integral equation [30] and decompose the contributions of the wave packets launched by the SAP with initial momenta along the positive and negative directions of the laser polarization axis, for the same laser parameters used in Fig. 1. We find that the PEs with $p_z < 0$ originate from (a) *direct ionization* of the PEs with initially negative momentum ($p_z(0) < 0$), (b) PEs with initially negative momenta that

are turned around by the IR-field and *backscatter* from the parent core, and (c) PEs that have initially positive momentum, that are turned around by the IR-field, and forward scatter from the ion. Figure 4(a) shows that the interference pattern at low energies originates mainly from the PEs (a) and (b). To confirm this, we produced a movie [31] of the PE wave packet which shows that the interference structure only appears during the second half-cycle of the IR field following ionization of the PE (cf. Fig. 1(a) inset). We also find that the backscattered part of the wave packet is opposite in sign to the directly ionized part. We find that the PEs with $p_z > 0$ originate primarily from (a) *direct ionization* of the PEs with initially positive momentum ($p_z(0) > 0$), and (b) PEs with initially negative momenta ($p_z(0) < 0$) that drift back to the ion under the influence of the IR field and *forward scatter*. Figure 4(b) shows that the hump at low energies originates mainly from the forward-scattered PEs. To confirm this origin of the low-energy peak, we analyzed the time-dependent electron wave packet, which shows a return to, and subsequent exit from, a sphere around the parent ion [32].

In summary, we have investigated theoretically low-energy photoelectron spectra for ionization of an atom by a few-cycle SAP in the presence of an intense IR laser pulse, i.e., low-energy attosecond streaking. The interference patterns in the photoelectron spectra reveal the quantum trajectories of the continuum electrons. The IR laser field is shown to provide a remarkable degree of control over the continuum-electron dynamics in the low-energy region. A short IR laser pulse can guide some initially ionized electrons back to the parent ion from which they rescatter and interfere with directly ionized electrons, thus providing a kind of holographic imaging of the ionic potential. By increasing the IR laser pulse length, multiple

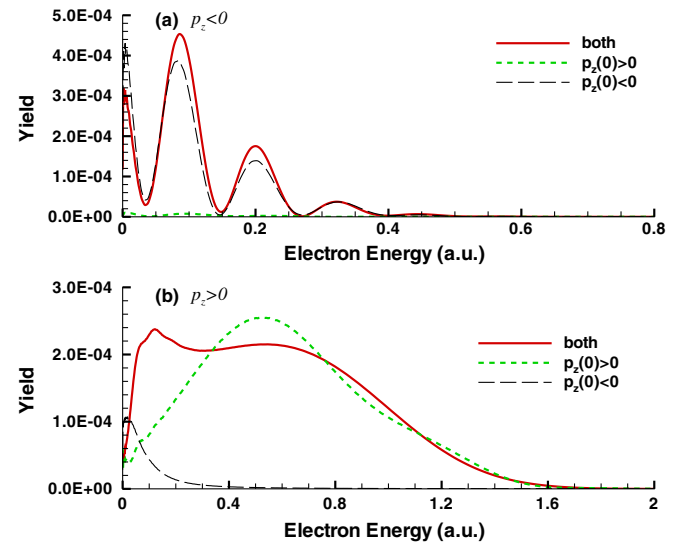


FIG. 4 (color online). Photoelectron spectra of He in combined SAP and IR fields for (a) negative and (b) positive momenta p_z . The SAP and IR laser parameters are the same as in Fig. 1.

returns of PEs have been shown to arise. Further control of electron dynamics in the continuum will require waveform shaping of the driving laser field, e.g., by adding a second harmonic of the fundamental IR laser. Although this proposed low-energy attosecond streaking is experimentally feasible at present, a full quantum-mechanical description of the process remains a theoretical challenge. The dynamics of low-energy continuum electrons is dominated by both the strong IR laser field and the ionic core potential. Thus any analytic quantum theory of low-energy attosecond streaking that neglects this potential (such as, e.g., [33]) cannot describe the low-energy PE spectrum. Any such theory must treat not only the IR laser field but also (multiple) scattering from the ionic potential.

We gratefully acknowledge fruitful discussions with T. Morishita and O. I. Tolstikhin. This work was supported by the National Natural Science Foundation of China under Grants No. 11174016, No. 10974007, No. 10821062, and by the U.S. Department of Energy under Grant No. DE-FG02-96ER14646. X. M. T. was supported by the Japan Society for the Promotion of Science.

*liangyou.peng@pku.edu.cn

†qhong@pku.edu.cn

‡tong@ims.tsukuba.ac.jp

§astarace1@unl.edu

- [1] K. J. Schafer, B. Yang, L. F. DiMauro, and K. C. Kulander, *Phys. Rev. Lett.* **70**, 1599 (1993).
- [2] P. B. Corkum, *Phys. Rev. Lett.* **71**, 1994 (1993).
- [3] T. Morishita, A.-T. Le, Z. Chen, and C. D. Lin, *Phys. Rev. Lett.* **100**, 013903 (2008).
- [4] M. Meckel *et al.*, *Science* **320**, 1478 (2008).
- [5] S. Haessler *et al.*, *Nature Phys.* **6**, 200 (2010).
- [6] T. Brabec, M. Yu. Ivanov, and P. B. Corkum, *Phys. Rev. A* **54**, R2551 (1996).
- [7] K. Schiessl, K. L. Ishikawa, E. Persson, and J. Burgdörfer, *Phys. Rev. Lett.* **99**, 253903 (2007).
- [8] P. Johnson *et al.*, *Phys. Rev. Lett.* **95**, 013001 (2005).
- [9] P. Johnsson, J. Mauritsson, T. Remetter, A. L’Huillier, and K. J. Schafer, *Phys. Rev. Lett.* **99**, 233001 (2007).
- [10] P. Rivière, O. Uhden, U. Saalmann, and J. M. Rost, *New J. Phys.* **11**, 053011 (2009).
- [11] P. Ranitovic *et al.*, *New J. Phys.* **12**, 013008 (2010).
- [12] M. B. Gaarde, C. Buth, J. L. Tate, and K. J. Schafer, *Phys. Rev. A* **83**, 013419 (2011).
- [13] K. R. Overstreet, R. R. Jones, and T. F. Gallagher, *Phys. Rev. Lett.* **106**, 033002 (2011).
- [14] P. Ranitovic *et al.*, *Phys. Rev. Lett.* **106**, 193008 (2011).
- [15] G. Sansone *et al.*, *Science* **314**, 443 (2006).
- [16] E. Goulielmakis *et al.*, *Science* **320**, 1614 (2008).
- [17] X. Feng *et al.*, *Phys. Rev. Lett.* **103**, 183901 (2009).
- [18] R. Kienberger *et al.*, *Science* **297**, 1144 (2002).
- [19] J. Itatani *et al.*, *Phys. Rev. Lett.* **88**, 173903 (2002).
- [20] M. Schultze *et al.*, *Science* **328**, 1658 (2010).
- [21] D. R. Hartree, *The Calculation of Atomic Structures* (Wiley, New York, 1957), §. 2.5.
- [22] H. G. Muller, *Laser Phys.* **9**, 138 (1999).
- [23] L.-Y. Peng, E. A. Pronin, and A. F. Starace, *New J. Phys.* **10**, 025030 (2008).
- [24] P. Salières *et al.*, *Science* **292**, 902 (2001).
- [25] In our classical simulations, we have neglected PEs with extremely low kinetic energies, which may experience multiple returns under the influence of the IR laser field.
- [26] The ac stark shift induced by the IR field increases the ionization potential by 1.05 eV, which is also taken into account.
- [27] C. I. Blaga *et al.*, *Nature Phys.* **5**, 335 (2009).
- [28] W. Quan *et al.*, *Phys. Rev. Lett.* **103**, 093001 (2009).
- [29] For the trapezoidal envelopes employed for the IR laser pulses, higher-order electron trajectories occur for shorter pulse durations than they do for smoother pulse envelope shapes.
- [30] X. M. Tong, K. Hino, and N. Toshima, *Phys. Rev. A* **74**, 031405(R) (2006).
- [31] See Supplemental Material at <http://link.aps.org/supplemental/10.1103/PhysRevLett.107.183001> for a movie of the PE wave packet vs time (measured in IR-field optical cycles).
- [32] X. M. Tong, S. Watahiki, K. Hino, and N. Toshima, *Phys. Rev. Lett.* **99**, 093001 (2007).
- [33] M. Kitzler, N. Milosevic, A. Scrinzi, F. Krausz, and T. Brabec, *Phys. Rev. Lett.* **88**, 173904 (2002).